An overview of the Magneto-Optic Kerr Effect

Audric Lemonnier*

Physics Department, Université Pierre-et-Marie-Curie (Paris 6), France

(Dated: May 6, 2016)

Abstract

The Magneto-Optical Kerr Effect (MOKE) is a powerful tool for studying the magnetic properties of ferromagnetic and ferrimagnetic thin films and multilayers, as mapping magnetics areas. This magnetometer is often preferred for its accuracy and ease of implementation, where other methods such as SQUID or Vibrating Sample Magnetometer (VSM) remain expensive and restrictive (low temperatures, samples deterioration, time for acquisition, *et cetera*). Researches in this field expanded significantly simultaneously with the ones led in the engineering of magneto-optical data storage. The reading head of magneto-optical drives uses the polar Kerr effect which offers the largest rotation. However, this technology seems to be obsolete. The purpose of this study is to highlight the Kerr effect after building a simple setup based on the equipment at our disposal. After a brief explanation of the MOKE, we will clarify some theoretical elements and will present our experiment. Then, we will compare the results of our setup with the professional one.

I. INTRODUCTION

The Kerr effect was discovered in 1877.[1] It appears when a linearly polarised electromagnetic wave is reflected on a metal surface in presence of an electric or magnetic field (MOKE). The polarization of the reflected wave becomes elliptical and the rotation of the polarization (few mrad) is proportional to both the magnetization $\mathbf{M}$ and the thickness of media. Its microscopic origin (Zeeman effect) is based on the spin-orbit interaction and relativistic effects.[2] We can notice a second effect in the magnetic case corresponding to the Voigt effect, generally ignored as it is very weak. Depending on the direction of $\mathbf{M}$ (Fig. 1), there are three geometric configurations of MOKE: polar, longitudinal, transverse. We must know that generally the observed effect is the superposition of the three MOKE modes. These effects are greater for materials with a particular symmetry which is reflected in the

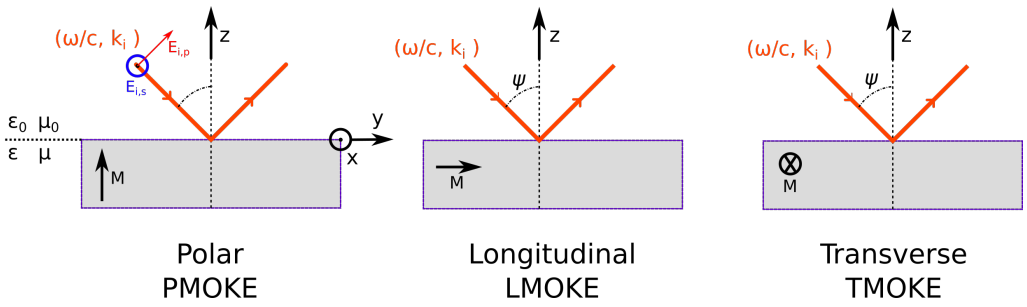

FIG. 1. Three geometries of MOKE.

form of its dielectric tensor. The properties of the dielectric tensor come from thermostatistic and is Hermitian in the absence of absorption in a magnetic medium.[3]

II. THEORY

In this section we explain theory of PMOKE but the other cases are similar. Consider a linearly polarized monochromatic wave in the visible range, with pulsation ω and wave number k, propagating in air and inciding perpendicularly on a ferromagnetic material. Its electric field is $E(t,z) \propto e^{-i(\omega t - kz)}$. We introduce the electric displacement $\mathbf{D}$ and the magnetic induction $\mathbf{B}$ linked to the magnetic field $\mathbf{H}$:

$$\forall\, i,j \in \{1,2,3\}, \quad \mathbf{D} = \boldsymbol{\varepsilon}\mathbf{E} = \varepsilon_0 \boldsymbol{\varepsilon_r}\mathbf{E} \iff D_i = \varepsilon_{ij}(\omega) E_j, \tag{1}$$

$$\mathbf{B} = \boldsymbol{\mu}\mathbf{H} = \mu_0(\mathbf{H}+\mathbf{M}) \iff B_i = \mu_{ij}(\omega) H_j, \tag{2}$$

where $\boldsymbol{\varepsilon}$, $\boldsymbol{\varepsilon_r}$ and $\boldsymbol{\mu}$ are the tensorial permittivity, relative permittivity and permeability. The permeability at optical frequencies is close to the vacuum permeability μ_0 for magnetic and non-magnetic media (Landau hypothesis).[3] Thus, we assume that $\mu_{ij} = \mu_0 \delta_{ij}$, where $\boldsymbol{\delta}$ is the Krönecker symbol. Assuming that the medium is electrically neutral, Maxwell equations give us:

$$\nabla \cdot \mathbf{D} = 0, \quad \nabla \times \mathbf{E} = -\partial_t \mathbf{B}, \quad \nabla \times \mathbf{H} = \mathbf{j} + \partial_t \mathbf{D}. \tag{3}$$

The current density $\mathbf{j}$ takes into account the conductivity tensor $\boldsymbol{\sigma}$: $\mathbf{j} = \boldsymbol{\sigma}\mathbf{E}$. We can define an effective permittivity $\boldsymbol{\varepsilon'} = \boldsymbol{\varepsilon} + i\dfrac{\boldsymbol{\sigma}}{\omega}$. Equations (3) allow to write :

$$\begin{aligned} \frac{1}{\mu_0}\nabla \times \partial_t \mathbf{B} = \partial_t \mathbf{j} + \partial_t^2 \mathbf{D} \;&\Leftrightarrow\; -\nabla \times \nabla \times \mathbf{E} = \omega^2 \mu_0 (i\frac{\boldsymbol{\sigma}}{\omega} + \boldsymbol{\varepsilon})\mathbf{E} \\ &\Leftrightarrow\; k^2 \mathbf{E} - (\mathbf{k} \cdot \mathbf{E})\mathbf{k} = \frac{\omega^2}{c^2}\boldsymbol{\varepsilon'}\mathbf{E}. \end{aligned}$$

This last equation can be reformulated by using the complex index $n_i = \dfrac{c}{\omega}k_i$:

$$(n^2 \delta_{ij} - n_i n_j - \varepsilon'_{ij}) E_i = 0. \tag{4}$$

The nonzero solution is given by zeros of the determinant of the prefactor and leads to the Fresnel formula for the calculation of normal modes of propagation.

We have to keep in mind the importance of off-diagonal terms which are functions of $\mathbf{M}$ and are the reason of the magneto-optic effect.[4] The dielectric tensor has to obey the Onsager reciprocal relation by magnetization reversal: $\varepsilon'_{ij}(\mathbf{M}) = \varepsilon'_{ji}(-\mathbf{M})$. Equation (4) simplifies if one makes additional hypothesis on the symmetries of the sample, like hexagonal symmetry (*id est* $\varepsilon'_{11} = \varepsilon'_{22} \neq \varepsilon'_{33}$).[6] If $\mathbf{M}$ is led parallel to an axis of $\boldsymbol{\varepsilon'}$, the tensor is invariant by rotation around this axis: $\varepsilon'_{12} = -\varepsilon'_{21}$. In PMOKE situation with z-axis collinear to $\mathbf{M}$, the permittivity tensor is :

$$\boldsymbol{\varepsilon'} = \begin{pmatrix} \varepsilon'_{xx} & \varepsilon'_{xy} & 0 \\ -\varepsilon'_{xy} & \varepsilon'_{xx} & 0 \\ 0 & 0 & \varepsilon'_{zz} \end{pmatrix}, \quad \varepsilon'_{xy} \in i\mathbb{R}.^{7} \tag{5}$$

The Fresnel equation becomes a second order equation in n^2, and yields zeros $n_\pm^2 = \varepsilon'_{xx} \pm i\varepsilon'_{xy}$ (assuming $n_x = 0$ and $n_y = 0$). The eigenmodes are found by replacing these eigenvalues in Eq. (4) and then, we can demonstrate that $E_x = \pm i E_y = e^{\pm i\frac{\pi}{2}} E_y$. This means that we have two waves with a circular polarization (left and right-handed), propagating with the index

n_+ and n_-. Induction is:

$$D_+ = n_+^2(E_x + iE_y), \quad D_- = n_-^2(E_x - iE_y). \tag{6}$$

Light is elliptical after reflection. Fresnel coefficients $r_{\bullet\bullet}$ for s and p of reflected field $\mathbf{E}_r$ are calculated with incident field $\mathbf{E}_i$ and boundary conditions on the interface. s or p denotes polarization when the electric field of the light is orthogonal or parallel to the plane of incidence. Starting from:

$$\begin{pmatrix} E_{r,p} \\ E_{r,s} \end{pmatrix} = \begin{pmatrix} r_{pp} & r_{ps} \\ r_{sp} & r_{ss} \end{pmatrix} \begin{pmatrix} E_{i,p} \\ E_{i,s} \end{pmatrix}, \tag{7}$$

we define Kerr rotation θ_{kerr} and Kerr helicity η_{kerr} for s and p lights for all MOKE modes:

$$\theta_{kerr,s} = \mathtt{Re}(\frac{r_{ss}}{r_{sp}}), \quad \eta_{kerr,s} = \mathtt{Im}(\frac{r_{ss}}{r_{sp}}), \tag{8}$$

$$\theta_{kerr,p} = \mathtt{Re}(\frac{r_{ps}}{r_{pp}}), \quad \eta_{kerr,p} = \mathtt{Im}(\frac{r_{ps}}{r_{pp}}).^{8} \tag{9}$$

In the next section we perform the measurement of the p and s components in LMOKE, with an incident polarization p. According to $E_{i,s} = 0$, Fresnel coefficients that interest us are:

$$r_{sp} = -i\frac{\beta Q_v \cdot n cos\,\psi}{(cos\,\psi + n\gamma)(n cos\,\psi + \gamma)\cdot\gamma}, \tag{10}$$

$$r_{pp} = \frac{n cos\,\psi - \gamma}{n cos\,\psi + \gamma}, \tag{11}$$

where n is the complex index, ψ is the angle of incidence, $(0, \beta, \gamma) = \frac{\mathbf{k}}{||\mathbf{k}||}$ the direction of the incident wave and $Q_v = i\frac{\varepsilon'_{xy}}{\varepsilon'_{xx}} \propto ||\mathbf{M}||$ the Voigt constant.[2]

III. EXPERIMENT

We performed a first LMOKE experiment on steel sample made of a cutter blade. Light from an unpolarized He-Ne laser 15mW goes through a polarizer (Polaroid) and is reflected on the sample under an external magnetic field (about 300mT) generated by two electromagnets. It goes through a Wollaston prism, splits the two orthogonal components which are detected by two photodiodes. Signals are then linearly amplified until the oscilloscope. Three problems arose. First, the light intensity fluctuates over time when an unpolarized He-Ne laser is polarized (due to the geometry of the cavity) and measurements are then

impossible.[5] The second problem is related to the size of the speckle ($\sim$ 5mm) on the sample, making it impossible to capture the whole flow of light on the photodiodes. Finally the angle of incidence is weakly adjustable ($\pm$5 deg.).

We built better LMOKE, PMOKE and TMOKE setups with cobalt sandwiched between two layer of titanium oxide and a silicon substrate Si(100)/TiO_2/Co/TiO_2 (4nm of Co thickness) with a linearly polarized laser diode and two 200mm lens for beam focus, as shown in Fig. 2. We were unable to adjust the angle of incidence due to the electromagnets size, which is an unfortunate drawback as the angle for maximizing Kerr effect is not approachable. A Hall probe is arranged close to the sample in order to measure the field produced by the coils. We measure the relative shift of voltage as function of magnetic field for light with s and p polarizations. The detection of the Kerr effect is done by recording $\theta_{Kerr} \propto \dfrac{V_{ch1} - V_{ch2}}{V_{ch1} + V_{ch2}}$, with the change of polarization via the voltages of the photodiodes V_{ch1} and V_{ch2}, as function of the magnetic field adjusted with the rheostat.

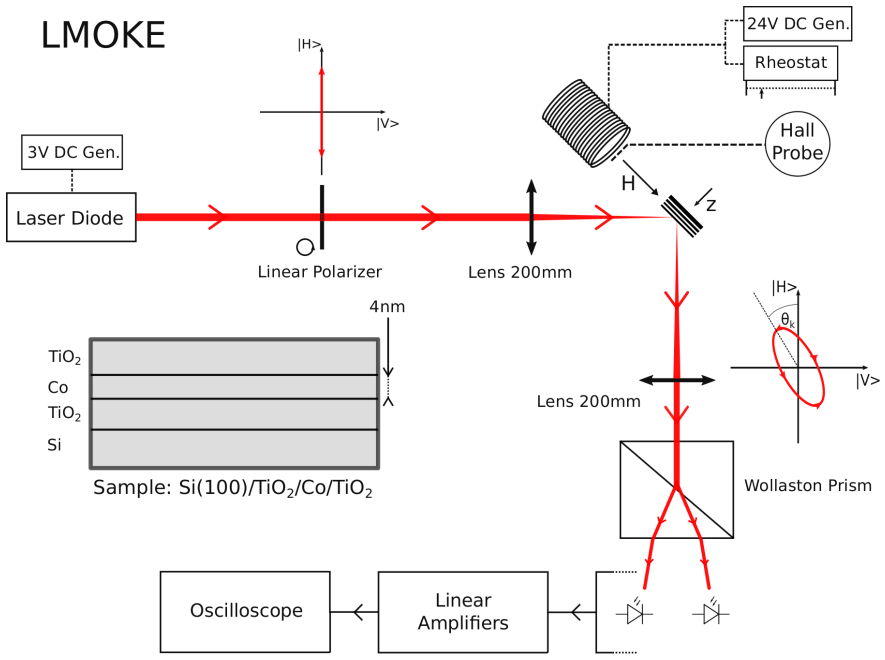

FIG. 2. The second setup.

IV. RESULTS AND DISCUSSION

The best raw result is presented in Fig. 3 for the LMOKE for an incident polarization p on the cobalt sample. The measurement was done over 45 minutes for a $\pm$37.0mT loop with

the diode giving the s and p components. Although, the Kerr effect is actually visible, it is not quantifiable. Moreover, the p component measurement has to be constant as shown in Eq. (11). We cannot link this graph to a cobalt hysteresis loop, nor see the coercive field. It is clear that problem comes from hardware and duration of the measurement:

- All optical elements are on a mobile support, the experiment is very sensitive to vibrations.
- Because of the duration of the measurement, the power of the laser diode varies. Electromagnets warm up and the heat is transmitted to the aluminum support on which the sample was put.
- The last problem is that amplifiers boxes are not electromagnetically shielded.

We had the opportunity to participate in acquisition of the loop of our sample with a different method at INSP's lab. This meeting was a way to know what to expect, and a way to compare our results. This experiment is built upon an optical table based on modulation techniques with the chain: Polarizer ▷ Sample ▷ Analyzer ▷ Photo-Elastic Modulator (PEM) ▷ Photodiode ▷ Lock-in Amplifier, as in Ref. 9. Data is exposed in Fig. 4 and seem having no correlation with our measures, in particular due to the high sensitivity of the angle of incidence.

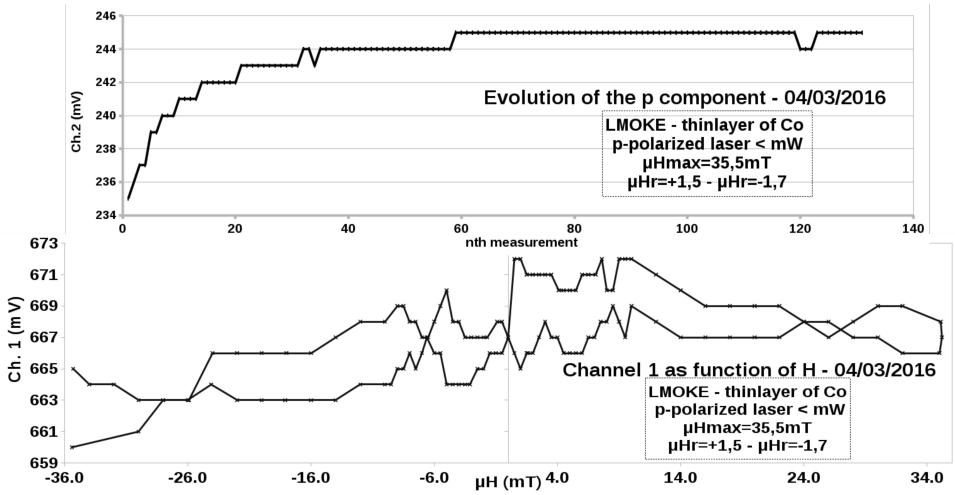

FIG. 3. p-LMOKE loop Co in 45min (bottom) and evolution of the p component detected (top).

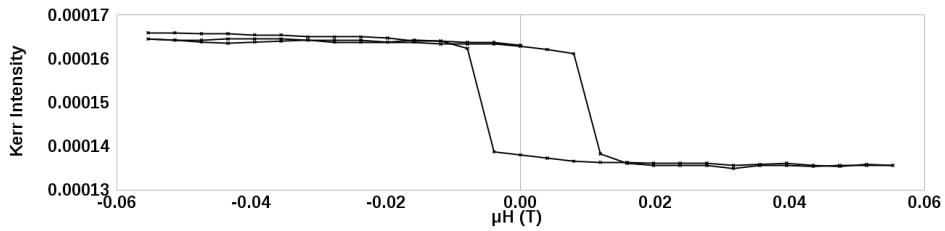

FIG. 4. LMOKE loop Co in 10s at INSP.

V. CONCLUSION

One of two major steps in the development of such application is the determination of the equation of normal modes, but it rises no difficulties. Once known, we determine reflection coefficients. We cannot do more with this formalism, but it is sufficient for understanding this effect. For more refinement, the Kubo equation, the Argyres treatment and the Drude-Lorentz model are needed in order to understand the conductivity tensor and how off-diagonal terms of dielectric tensor are linked to magnetization.[10,11] This quantum study is beyond our framework.

We were only able to highlight the effect in the allotted time. This kind of MOKE experiment as simple as it can be needs very good optical and measurement components. It would have been more interesting to obtain the cobalt hysteresis loop in the three configurations: for several wavelengths, for different angles of incidence and at saturation. The cost of an experimental setup on optical table can be estimated at more than several tens of thousands euros, like the one at INSP's lab, and requires synchronous detection skills.

ACKNOWLEDGMENTS

We gratefully acknowledge Dr. Franck Vidal (INSP) for his advices, the loan of the cobalt sample and the data acquisition with his research experiment.

---

* audric.lemonnier@etu.upmc.fr

[1] J. Kerr, "On rotation of the plane of polarization by reflection from the pole of a magnet", Philos. Mag. **3** (1877).

[2] E. du Trémolet de Lacheisserie, *Magnétisme T. 1*, (EDP Sciences, 2000), pp. 401-406.

[3] L. Landau, E. Lifchitz, *Electrodynamics of continious media T. 8*, (Pergamon Press, 1960), §82.

[4] Y. Hinschberger Schreiber, "Etude théorique des effets relativistes induits par une impulsion lumineuse ultra-rapide dans la matière", IPCMS (2012), Ph.D dissertation.

[5] Sextant, *Optique expérimentale*, (Hermann, 1997), Ch. IV.7.

[6] Wikipedia website about cobalt (structure cristalline), `https://fr.wikipedia.org/wiki/Cobalt`.

[7] V. Antonov, B. Harmon, A. Yaresko, *Electronic Structure and Magneto-Optical Properties of Solids*, (Kluwer Academic Publishers, 2004), §1.4.2..

[8] Chun-Yeol You, Sung-Chul Shin, "Derivation of simplified analytic formulae for magneto-optical Kerr effects", Appl. Phys. Lett. **69** (1315).

[9] S. Polisetty, J. Scheffler, S. Sahoo, Yi Wang, T. Mukherjee, Xi He, Ch. Binek, "Optimization of magneto-optical Kerr setup", Rev. Sci. Instrum. **79** (5).

[10] P. N. Argyres, "Theory of the Faraday and Kerr Effects in Ferromagnetics" , Phys. Rev. **97** (334) (1955).

[11] M. Inoue, M. Levy, A. V. Baryshev, *Magnetophotonics: From theory to Applications*, (Springer, 2013).